Numerically Stable Moment Matching for Linear Systems Parameterized by Polynomials in Multiple Variables with Applications to Finite Element Models of Microwave Structures

Ortwin Farle, and Romanus Dyczij-Edlinger, *Member, IEEE,*

***Abstract*—Nowadays, model order reduction is not only used for fast frequency sweeps, but increasingly applied to systems exhibiting additional parameters like material properties and geometry parameters. Existing order reduction approaches for the hereby often emerging multivariate polynomially parameterized systems still lack the numerical stability of single-parameter methods. In this paper we present a novel multi-parameter algorithm with the same numerical robustness as the well established single-parameter approaches. Compared to existing methods, additional key features are a reduced memory consumption, a straightforward parallelization, and an increased flexibility in handling non-uniform parameters ranges.**

***Index Terms*—Finite element methods, reduced order systems.**

I. Introduction

AMONG the various numerical electromagnetic techniques, the finite element method (FEM) is one of the most versatile in handling arbitrary material properties and geometric shapes. During a design cycle or a parametric study, a process of repeated simulation alternating with changing of the parameters is performed. Due to the large number of simulations, the high computational times often prevent a sufficiently dense sampling of parameter space. This is especially true, when multiple parameters are involved. As a possible solution to this problem, model order reduction (MOR) techniques have recently been extended from the single parameter [1] to the multiple parameter case [2], [3], [4]. Order reduction is a well established methodology in the electromagnetic community for computing fast frequency sweeps [5]. In recent times additional parameters like incidence angles [6], wire spacings [7] and material properties are considered [8]. Most modern order reduction methods are of projection type, i.e. the original full model is projected onto a low dimensional subspace of appropriate global shape functions. The proposed methods mainly differ in the choice of projection basis. They can be classified as either single-point or multi-point methods. Single-point methods are usually of moment-matching type, this means the transfer function and its derivatives up to a certain order are identical for the reduced order model (ROM) and the original model at a chosen expansion point. As long as the FE system can be factorized, single-point methods are very attractive since they usually require only one matrix factorization and several matrix-vector multiplications and forward and back substitutions. Multi-point methods come along with the need for a separate matrix factorization at each expansion point, which can be extremely time consuming.

The direct computation of the moments to achieve moment-matching is with rising order increasingly ill-conditioned. For single-parameter systems this problem has been solved with the advent of Krylov methods, first for linear parameterization [9], and finally for polynomial parameterization [10], [11]. The latter was possible by extending the notion of Krylov subspaces to higher order. The generalization of the numerically stable Krylov subspace methods from the single to the multiparameter case is up to now not fully solved, since the multiparameter methods still don't feature the same degree of numerical robustness. Therefore, most of the proposed methods avoid the difficulties by resorting to multipoint methods [6], where only moments of low order are considered at each expansion point. In [12] it is proposed to discard the mix terms and only take the terms along the coordinate axes into account. This allows the use of numerically robust single-point methods along the coordinate axes. Even though this approach may lead to good results for certain practical applications, in [8], Sec. III, A. a system is presented, for which this method will certainly fail. The authors of [13] solve the problem of numerical robustness for linear parameterization by considering a superspace of the sought projection space. Its special structure allows the stable computation of a basis by using the Arnoldi algorithm. Since more projection vectors are computed than are really needed for matching the moments, this method requires additional numerical costs for ROM generation and evaluation. In [14], a generalization of the Arnoldi algorithm is presented. Even though this approach allows a stable computation along one parameter axis, the computation of moments along other axes still suffers from numerical cancelation. This reduces the applicability of the method to the case where the parameter space is broadband along one parameter and only minor parameter changes along other directions are considered. Another interesting approach for dealing with the numerical stability problem is given in [15]. It is shown, how the construction of the multiparameter projection basis can be reduced in the multilinear case to a sequence of properly chosen single-parameter sweeps. One popular way to apply algorithms developed for multilinear

The authors are with Lehrstuhl für Theoretische Elektrotechnik, Saarland University, Campus, D-66123, Germany (e-mail: o.farle@lte.uni-saarland.de)

Manuscript received April 19, 2005; revised January 11, 2007.

parameterization to polynomial parameterization, is to linearize the polynomial problem, and so replace the original system by a much larger system. With increasing polynomial degree this can lead to prohibitive memory consumption and computational costs, and should therefore be avoided. To the authors' knowledge, the only method capable of directly handling polynomially parameterized systems in a numerically robust way, is the algorithm presented in [16]. Even though this method performs quite well in the vast majority of cases, it is still a kind of QR-factorization of the multivariate Krylov space, which may lead to numerical instabilities at high moment orders.

In this paper we will present a generalization of [10] to multi-parameter systems. By reducing the multi-parameter case to the single-parameter case, our approach inherits the numerical robustness from the single-parameter method. Compared to existing approaches further advantages of the new algorithm are reduced memory consumption, improved runtime, a straightforward parallelization, and the possibility to easily deal with non-uniform parameter ranges. Before describing the new algorithm, we first analyze in Section III the projection spaces for moment-matching order reduction of multivariate polynomially parameterized systems. Existing proofs [3] for the moment-matching property of the ROMs only consider one sided methods and do not take parameterization of the input and output vectors into account. Our proof doesn't show these restrictions.

II. Preliminaries

We employ multi-index notation with the usual conventions

$$\alpha = (\alpha_1, \alpha_2, \dots, \alpha_m) \qquad \alpha! = \prod_{i=1}^{m} \alpha_i! \quad |\alpha| = \sum_{i=1}^{m} \alpha_i \tag{1}$$

$$\mathbf{s} = [s_1 \ s_2 \ \dots \ s_m]^T \qquad \mathbf{s}^\alpha = \prod_{i=1}^{m} s_i^{\alpha_i} \tag{2}$$

$$D^\alpha = \frac{\partial^{|\alpha|}}{\partial s_1^{\alpha_1} \dots \partial s_m^{\alpha_m}} \tag{3}$$

$$\mathbf{x}_\alpha = \mathbf{0} \qquad \text{if } \exists i \in \{1, \dots, m\} : \ \alpha_i < 0. \tag{4}$$

We consider the single-input, single-output (SISO) system

$$\mathbf{A}(\mathbf{s})\mathbf{x}(\mathbf{s}) = \mathbf{b}(\mathbf{s})u(\mathbf{s}) \tag{5a}$$

$$y(\mathbf{s}) = \mathbf{c}^T(\mathbf{s})\mathbf{x}(\mathbf{s}) \tag{5b}$$

whose system matrix $\mathbf{A}(\mathbf{s})$, right-hand side $\mathbf{b}(\mathbf{s})$, and output functional $\mathbf{c}(\mathbf{s})$ are parameterized by polynomials of maximum degree M in m scalar parameters $s_1, s_2, \dots, s_m \in \mathbb{C}$,

$$\mathbf{A}(\mathbf{s}) = \sum_{|\alpha|=0}^{|\alpha|\le M} \mathbf{s}^\alpha \mathbf{A}_\alpha \quad \mathbf{b}(\mathbf{s}) = \sum_{|\alpha|=0}^{|\alpha|\le M} \mathbf{s}^\alpha \mathbf{b}_\alpha \quad \mathbf{c}(\mathbf{s}) = \sum_{|\alpha|=0}^{|\alpha|\le M} \mathbf{s}^\alpha \mathbf{c}_\alpha \tag{6}$$

with $\alpha_i \ge 0$, $\mathbf{A}_\alpha \in \mathbb{C}^{N\times N}$, and $\mathbf{x}, \mathbf{b}_\alpha, \mathbf{c}_\alpha \in \mathbb{C}^N$. Since we are mainly interested in the transfer function $H(\mathbf{s}) : u(\mathbf{s}) \mapsto y(\mathbf{s})$, we assume without loss of generality that $u = 1$ and just deal with a simplified system Σ, given by

$$\Sigma(\mathbf{s}): \quad \mathbf{A}(\mathbf{s})\mathbf{x}(\mathbf{s}) = \mathbf{b}(\mathbf{s}) \tag{7a}$$

$$H(\mathbf{s}) = \mathbf{c}^T(\mathbf{s})\mathbf{x}(\mathbf{s}) = \mathbf{c}^T(\mathbf{s})\mathbf{A}^{-1}(\mathbf{s})\mathbf{b}(\mathbf{s}). \tag{7b}$$

The *Taylor series* of $H(\mathbf{s})$ about the origin is defined by

$$H(\mathbf{s}) = \sum_{|\alpha|=0}^{\infty} m_\alpha \mathbf{s}^\alpha \qquad m_\alpha \in \mathbb{C} \tag{8}$$

wherein the *moments* m_α are given by

$$m_\alpha = \frac{1}{\alpha!} D^\alpha H(\mathbf{s})\big|_{\mathbf{s}=\mathbf{0}}. \tag{9}$$

Similarly, the solution vector $\mathbf{x}$ of (7a) can be expanded in a Taylor series

$$\mathbf{x}(\mathbf{s}) = \sum_{|\beta|=0}^{\infty} \mathbf{x}_\beta \mathbf{s}^\beta \qquad \mathbf{x}_\beta \in \mathbb{C}^N. \tag{10}$$

Lemma 1. *Given a system of linear equations of the form* (7a) *and the Taylor series expansion of the solution vector* (10)*, the vector-valued Taylor coefficients $\mathbf{x}_\beta$ satisfy the recursion*

$$\mathbf{x}_\beta = \mathbf{A}_{\alpha=0}^{-1}\Big(\mathbf{b}_\beta - \sum_{|\alpha|=1}^{|\alpha|\le M} \mathbf{A}_\alpha \mathbf{x}_{\beta-\alpha}\Big). \tag{11}$$

The number of vectors $\mathbf{x}_\beta$ with $|\beta| \le q$ is

$$D_q = \sum_{k=0}^{q} \binom{k+m-1}{k}. \tag{12}$$

Proof of (11)*:* See Appendix A. ∎
Proof of (12)*:* By induction; see [7]. ∎

III. Projection Spaces for Reduced-Order Models

Definition 2. *A* projection-based ROM $\tilde{\Sigma}$ *of* (7) *is defined by*

$$\tilde{\Sigma}(\mathbf{s}): \quad \tilde{\mathbf{A}}(\mathbf{s})\tilde{\mathbf{x}}(\mathbf{s}) = \tilde{\mathbf{b}}(\mathbf{s})u(\mathbf{s}) \tag{13a}$$

$$\tilde{H}(\mathbf{s}) = \tilde{\mathbf{c}}^T(\mathbf{s})\tilde{\mathbf{x}}(\mathbf{s}) = \tilde{\mathbf{c}}^T(\mathbf{s})\tilde{\mathbf{A}}^{-1}(\mathbf{s})\tilde{\mathbf{b}}(\mathbf{s}) \tag{13b}$$

with

$$\tilde{\mathbf{A}}(\mathbf{s}) = \sum_{|\alpha|=0}^{|\alpha|\le M} \mathbf{s}^\alpha \tilde{\mathbf{A}}_\alpha \quad \tilde{\mathbf{b}}(\mathbf{s}) = \sum_{|\alpha|=0}^{|\alpha|\le M} \mathbf{s}^\alpha \tilde{\mathbf{b}}_\alpha \quad \tilde{\mathbf{c}}(\mathbf{s}) = \sum_{|\alpha|=0}^{|\alpha|\le M} \mathbf{s}^\alpha \tilde{\mathbf{c}}_\alpha. \tag{14}$$

Herein, $\tilde{\mathbf{A}}_\alpha$, $\tilde{\mathbf{b}}_\alpha$, and $\tilde{\mathbf{c}}_\alpha$ are given by

$$\tilde{\mathbf{A}}_\alpha := \mathbf{W}^T \mathbf{A}_\alpha \mathbf{V} \tag{15a}$$

$$\tilde{\mathbf{b}}_\alpha := \mathbf{W}^T \mathbf{b}_\alpha \tag{15b}$$

$$\tilde{\mathbf{c}}_\alpha := \mathbf{V}^T \mathbf{c}_\alpha \tag{15c}$$

with trial and test matrices $\mathbf{V}, \mathbf{W} \in \mathbb{C}^{N\times n}$, and $n \ll N$.

The Taylor series expansions of the reduced-order solution vector $\tilde{\mathbf{x}}$ and transfer function $\tilde{H}$ read

$$\tilde{\mathbf{x}}(\mathbf{s}) = \sum_{|\beta|=0}^{\infty} \tilde{\mathbf{x}}_\beta \mathbf{s}^\beta \qquad \tilde{\mathbf{x}}_\beta \in \mathbb{C}^n \tag{16}$$

$$\tilde{H}(\mathbf{s}) = \sum_{|\beta|=0}^{\infty} \tilde{m}_\beta \mathbf{s}^\beta \qquad \tilde{m}_\beta \in \mathbb{C} \tag{17}$$

and the corresponding errors $\mathbf{e_x}(\mathbf{s})$ and $e_H(\mathbf{s})$ are given by

$$\mathbf{e_x}(\mathbf{s}) = \mathbf{V}\tilde{\mathbf{x}}(\mathbf{s}) - \mathbf{x}(\mathbf{s}) \tag{18}$$

$$e_H(\mathbf{s}) = \tilde{H}(\mathbf{s}) - H(\mathbf{s}). \tag{19}$$

Obviously, the quality of the ROM depends strongly on the choice of $\mathbf{V}$ and $\mathbf{W}$. The following Lemma and Corollary address the construction of $\mathbf{V}$, and the resulting error:

Lemma 3. *Given a ROM after Definition 2 with*

$$\det(\mathbf{W}^T\mathbf{A}_{\alpha=0}\mathbf{V}) \neq 0. \tag{20}$$

If the trial matrix $\mathbf{V}$ is chosen such that

$$\operatorname{span}\Big\{\bigcup_{|\beta|=0}^{|\beta|\leq q}\mathbf{x}_\beta\Big\} \subseteq \operatorname{colsp}\{\mathbf{V}\} \tag{21}$$

the ROM matches the leading Taylor coefficients of the original system $\mathbf{x}_\beta$ up to order q, in the sense that

$$\mathbf{x}_\beta = \mathbf{V}\tilde{\mathbf{x}}_\beta \qquad \forall\beta : |\beta| \leq q. \tag{22}$$

Proof: See Appendix B. ■

Corollary 4. *For the ROM of Lemma 3, the errors in solution vector $\mathbf{x}(\mathbf{s})$ and transfer function $H(\mathbf{s})$ are of order $q+1$,*

$$\|\mathbf{e_x}(\mathbf{s})\| = \mathcal{O}(\mathbf{s}^\beta) \qquad \textit{with } |\beta| = q+1 \tag{23}$$

$$\|e_H(\mathbf{s})\| = \mathcal{O}(\mathbf{s}^\beta) \qquad \textit{with } |\beta| = q+1. \tag{24}$$

Proof of (23)*:* By plugging (22) into expansion (10). ■

Proof of (24)*:* $|e_H| = |\mathbf{c}^T\mathbf{e}_x| \leq \|\mathbf{c}\|\ \|\mathbf{e}_x\|$. ■

Note that Lemma 3 and Corollary 4 hold under the very weak assumption (20) on $\mathbf{W}$. Loosely speaking, we have achieved moment-matching up to order q (24) solely by an appropriate selection of the trial space $\operatorname{colsp}\mathbf{V}$.

In the following, we will show that, by a judicious choice of the testing space $\operatorname{colsp}\mathbf{W}$, the order of the error in the transfer function can be doubled. For this purpose, we introduce the *transposed system* Σ^T,

$$\Sigma^T: \quad \mathbf{A}^T(\mathbf{s})\mathbf{z}(\mathbf{s}) = \mathbf{c}(\mathbf{s}) \tag{25a}$$

$$K(\mathbf{s}) = \mathbf{b}^T(\mathbf{s})\mathbf{z}(\mathbf{s}) = \mathbf{b}^T(\mathbf{s})\mathbf{A}^{-T}(\mathbf{s})\mathbf{c}(\mathbf{s}). \tag{25b}$$

A comparison to (7b) shows that the transfer function $K(\mathbf{s})$ is the same as that of the original system (7):

$$K(\mathbf{s}) = K^T(\mathbf{s}) = H(\mathbf{s}). \tag{26}$$

In analogy to (10) and (11), the Taylor series expansion of $\mathbf{z}(\mathbf{s})$ and associated Taylor coefficients $\mathbf{z}_\beta$ are given by

$$\mathbf{z}(\mathbf{s}) = \sum_{|\beta|=0}^{\infty}\mathbf{z}_\beta\mathbf{s}^\beta \tag{27}$$

$$\mathbf{z}_\beta = \mathbf{A}_{\alpha=0}^{-T}\Big(\mathbf{c}_\beta - \sum_{|\alpha|=1}^{|\alpha|\leq M}\mathbf{A}_\alpha^T\mathbf{z}_{\beta-\alpha}\Big). \tag{28}$$

We are now ready to present the main result of this Section:

Theorem 5. *Given a ROM after Definition 2 with*

$$\det(\mathbf{W}^T\mathbf{A}_{\alpha=0}\mathbf{V}) \neq 0. \tag{29}$$

If the trial and test matrices $\mathbf{V}$ and $\mathbf{W}$ are chosen such that

$$\operatorname{span}\Big\{\bigcup_{|\beta|=0}^{|\beta|\leq q}\mathbf{x}_\beta\Big\} \subseteq \operatorname{colsp}\{\mathbf{V}\} \tag{30a}$$

$$\operatorname{span}\Big\{\bigcup_{|\beta|=0}^{|\beta|\leq p}\mathbf{z}_\beta\Big\} \subseteq \operatorname{colsp}\{\mathbf{W}\} \tag{30b}$$

where $\mathbf{x}_\beta$ and $\mathbf{z}_\beta$ are the Taylor coefficients of (11) *and* (28)*, respectively, the ROM matches the leading moments of the original model $m_\beta(\mathbf{s}=\mathbf{0})$ up to order $q+p+1$,*

$$m_\beta = \tilde{m}_\beta \qquad \forall\beta:\ |\beta| \leq q+p+1 \tag{31}$$

and the error in the transfer function is of order $q+p+2$,

$$|e_H| = \mathcal{O}(\mathbf{s}^\beta) \qquad \textit{with } |\beta| = q+p+2. \tag{32}$$

Proof of (31)*:* See Appendix C. ■

Proof of (32)*:* By plugging (31) into expansion (8). ■

A few remarks are in order:

Remark 6. Theorem 5 generalizes the results of [XXX] to two-sided projections and parameter-dependent right-hand sides $\mathbf{b}(\mathbf{s})$ and output functionals $\mathbf{c}(\mathbf{s})$.

Remark 7. By setting $\operatorname{colsp}\mathbf{V} = \operatorname{span}\mathbf{x}_\beta$ and $\operatorname{colsp}\mathbf{W} = \operatorname{span}\mathbf{z}_\beta$ in (30), it can be seen that the maximum order of the moments a ROM of dimension D_q can match is $2q+1$.

Remark 8. Since the Taylor coefficients $\mathbf{x}_\beta$ and $\mathbf{z}_\beta$ are utilized to construct the projection matrices $\mathbf{V}$ and $\mathbf{W}$ in (21) and (30), and because $\tilde{H}(\mathbf{s})$ matches the leading moments of the underlying transfer function $H(\mathbf{s})$ about the origin (31), one might mistake $\tilde{H}(\mathbf{s})$ as the Taylor expansion of $H(\mathbf{s})$. This is not the case. Rather, we have from (13b):

$$\tilde{H}(\mathbf{s}) = \Big(\sum_{|\alpha|=0}^{|\alpha|\leq M}\mathbf{s}^\alpha\tilde{\mathbf{c}}_\alpha^T\Big)\frac{\operatorname{adj}\Big(\sum_{|\alpha|=0}^{|\alpha|\leq M}\mathbf{s}^\alpha\tilde{\mathbf{A}}_\alpha\Big)}{\det\Big(\sum_{|\alpha|=0}^{|\alpha|\leq M}\mathbf{s}^\alpha\tilde{\mathbf{A}}_\alpha\Big)}\Big(\sum_{|\alpha|=0}^{|\alpha|\leq M}\mathbf{s}^\alpha\tilde{\mathbf{b}}_\alpha\Big). \tag{33}$$

With $\operatorname{adj}(\cdot)$ and $\det(\cdot)$ being polynomials in $\mathbf{s}$, $\tilde{H}$ becomes a rational function of the parameters. Due to the moment-matching property (31), we conclude that the reduced-order transfer function $\tilde{H}(\mathbf{s})$ is a multi-variate Padé approximation about the origin [17].

IV. Robust Computation of Projection Spaces

According to Section III, the projection matrices $\mathbf{V}$ and $\mathbf{W}$ are to span the linear hull of the multi-variate Taylor coefficients $\mathbf{x}_\beta$ and $\mathbf{z}_\beta$, which in turn are defined by (11) and (28). The structure of these recursions reveals that, once the factorization of the system matrix at the expansion point is available, all that is required to compute $\mathbf{x}_\beta$ or $\mathbf{z}_\beta$ is one forward-back substitution and a number of matrix-vector multiplications. Hence, single-point ROMs can be constructed very efficiently. However, implementing the recursions (11) and (28) directly would result in severe cancellation and make for an unreliable algorithm. This can easily be seen from the simple case of linear dependence on a single parameter with constant $\mathbf{b}$ and $\mathbf{c}$: then, (11) and (28) degenerate to the power

method, which strongly amplifies components in the directions of the dominant eigenvectors.

To overcome this difficulty, we propose to generalize the approach of [15] to the polynomial case: the overall idea is to choose appropriate directions in parameter space, construct single-parameter ROMs along these directions by proven methods, and recombine them to a multi-variate ROM. Here are the details:

Definition 9. *The* contraction $\Sigma(\mathbf{s})\big|_{\mathbf{p}}$ *denotes the linear system with polynomial dependence on a scalar parameter* $\epsilon \in \mathbb{C}$ *obtained by setting* $\mathbf{s}=\epsilon\mathbf{p}$ *in the multi-parameter system* $\Sigma(\mathbf{s})$.

Lemma 10. *The contraction* $\Sigma(\mathbf{s})\big|_{\mathbf{p}}$ *takes the form*

$$\Big(\sum_{i=0}^{i\le M}\epsilon^i\mathbf{A}_i\Big)\mathbf{x}(\epsilon)=\sum_{i=0}^{i\le M}\epsilon^i\mathbf{b}_m \tag{34a}$$

$$H(\epsilon)=\sum_{i=0}^{i\le M}\epsilon^i\mathbf{c}_i^T\mathbf{x}(\epsilon) \tag{34b}$$

wherein

$$\mathbf{A}_i=\sum_{|\alpha|=i}\mathbf{p}^\alpha\mathbf{A}_\alpha \quad \mathbf{b}_i=\sum_{|\alpha|=i}\mathbf{p}^\alpha\mathbf{b}_\alpha \quad \mathbf{c}_i=\sum_{|\alpha|=i}\mathbf{p}^\alpha\mathbf{c}_\alpha. \tag{35}$$

Proof: By plugging $\mathbf{s}=\epsilon\mathbf{p}$ into (7) and collecting terms of same power of ϵ. ■

========== End Roman ==========

Representation (10) implies that for $\epsilon \in \mathbb{C}$ and $\mathbf{p} \in \mathbb{C}^m$, the r-th derivative of $\mathbf{x}(\mathbf{s})$ in direction $\mathbf{p}$ is given by

$$\left.\frac{\mathrm{d}^r\mathbf{x}(\epsilon\mathbf{p})}{\mathrm{d}\epsilon^r}\right|_{\epsilon=0}=r!\sum_{|\beta|=r}\mathbf{x}_\beta\mathbf{p}^\beta. \tag{36}$$

It is important to notice that the right-hand side of (36) is a homogeneous polynomial in $\mathbf{p}$. The left-hand side corresponds to the r-th derivative of the solution vector of the univariate parameterized linear system of equations

$$\left(\sum_{|\alpha|=0}^{|\alpha|\le M}\epsilon^{|\alpha|}\mathbf{p}^\alpha\mathbf{A}_\alpha\right)\mathbf{x}(\mathbf{s})=\sum_{|\alpha|=0}^{|\alpha|\le M}\epsilon^{|\alpha|}\mathbf{p}^\alpha\mathbf{b}_\alpha \tag{37}$$

where ϵ is the parameter.

A. Reduction to single-parameter systems

We now relate the space spanned by (11) to the Taylor coefficients of a sequence of single parameter systems. In the following, we denote with $\mathcal{P}_r(\mathbf{s})$ the space of homogeneous polynomials of degree r in $\mathbf{s} \in \mathbb{C}^m$. Its dimension is given by

$$\dim\mathcal{P}_r(\mathbf{s})=\binom{r+m-1}{r}. \tag{38}$$

In the representation

$$\mathbf{x}(\mathbf{s})=\mathbf{x}_0+\sum_{|\beta|=1}\mathbf{x}_\beta\mathbf{s}^\beta+\ldots+\sum_{|\beta|=m}\mathbf{x}_\beta\mathbf{s}^\beta+\ldots \tag{39}$$

of the Taylor series (10), the r-th term is a homogeneous polynomial of degree r in $\mathbf{s}$. The coefficients $\mathbf{x}_\beta$ with $|\beta|=r$ are therefore uniquely determined by the univariate Taylor coefficients of contractions (37), if the set $\mathcal{S}_r=\{\mathbf{p}_i\}$ of directions is *unisolvent* in $\mathcal{P}_r(\mathbf{s})$. So we are able to state the following theorem:

Theorem 11. *Let* $\Sigma(\mathbf{s})$ *denote the multi-parameter system* (7)*,* $\mathbf{x}_\beta$ *its Taylor coefficients,* $\Sigma(\mathbf{s})\big|_{\mathbf{p}}$ *the contraction of* $\Sigma(\mathbf{s})$ *in direction* $\mathbf{p}$*, and* $\mathbf{x}_r(\mathbf{p})$ *the Taylor coefficient of degree* r *of* $\Sigma(\mathbf{s})\big|_{\mathbf{p}}$*. If the set of contraction directions* $\mathbf{p} \in \mathcal{S}_r$ *is unisolvent in* $\mathcal{P}_r(\mathbf{s})$*, the following statement holds:*

$$\operatorname{span}\left\{\mathbf{x}_\beta\big||\beta|=r\right\}=\operatorname{span}\left\{\mathbf{x}_r(\mathbf{p})\big|\mathbf{p}\in\mathcal{S}_r\right\}. \tag{40}$$

The importance of Theorem 11 lies in the fact that the computation of a basis of the linear hull of $\mathbf{x}_\beta$ can now be reduced to the computation of a basis of the linear hulls of the Taylor coefficients of a set of single-parameter systems $\Sigma(\mathbf{s})\big|_{\mathbf{p}}$. In this case, recursion (11) reduces to

$$\mathbf{x}_j=\mathbf{A}_0^{-1}\left(\mathbf{b}_j-\sum_{i=1}^{M}\mathbf{A}_i\mathbf{x}_{j-i}\right). \tag{41}$$

There exist several numerically stable algorithms to compute a basis of (41), see e.g. [10] and [11], which can now be applied to the multiparameter case. Note that for all contraction directions $\mathbf{p}$ the same $\mathbf{A}_0^{-1}$ is used. This implies that $\mathbf{A}_0$, in our case the FE system matrix in the expansion point, only has to be factorized once.

B. Algorithmic Implementation

To reuse information of lower orders it is advantageous to utilize a *hierarchical* set of contraction directions

$$\mathcal{S}_0\subset\mathcal{S}_1\subset\cdots\subset\mathcal{S}_r\subset\cdots\subset\mathcal{S}_q \tag{42}$$

where each set $\mathcal{S}_r$ is unisolvent in $\mathcal{P}_r(\mathbf{s})$, and q denotes the maximum order. In [15] the following choice was proposed

$$\mathcal{S}_r=\left\{(\gamma,q-|\gamma|)\;\middle|\;|\gamma|\le r\right\},\qquad r=0,\ldots,q \tag{43}$$

where γ is a multi-index of dimension $m-1$.

To compute a numerically stable basis $\{\mathbf{u}_0\ldots\mathbf{u}_q\}$ of the space of univariate Taylor coefficients, we use the WCAWE algorithm [10], because it can handle system matrices and right-hand sides of arbitrary polynomial degree. In the following, we introduce for this step the abbreviation

$$\begin{bmatrix}\mathbf{u}_0 & \ldots & \mathbf{u}_q\end{bmatrix}=\mathrm{WCAWE}\left(\Sigma(\mathbf{s})\big|_{\mathbf{p}},q\right). \tag{44}$$

Our proposed method for computing an orthonormal basis of (30a) is given in Alg. 1. In line 3 and line 4 we consider in each contraction direction an independent single-parameter model, which immediately allows a parallelization of the method. The vectors $\mathbf{u}_k(\mathbf{p})$ with $\mathbf{p}\notin\mathcal{S}_k$ are linearly dependent to the already computed basis $\mathbf{V}$ and are therefore discarded in line 6. In line 7 we use the modified Gram-Schmidt process (MGS) to ensure the orthonormality of matrix $\mathbf{V}$. Note that compared to [16] no additional auxiliary vectors have to be kept in memory.

Algorithm 1 Proposed Algorithm - Parallel Version

1: $\mathbf{V} = [\,]$
2: **for** $\forall \mathbf{p} \in \mathcal{S}_q$ **do**
3: Compute $\Sigma(\mathbf{s})\big|_{\mathbf{p}}$ according to (34a)
4: $[\mathbf{u}_0 \dots \mathbf{u}_q] = \mathrm{WCAWE}\left(\Sigma(\mathbf{s})\big|_{\mathbf{p}}, q\right)$
5: **for** $k := 0 \dots q$ **do**
6: **if** $\mathbf{p} \in \mathcal{S}_k$ **then**
7: $\mathbf{v} := \mathrm{MGS}\left(\mathbf{u}_k, \mathbf{V}\right)$
8: $\mathbf{V} := [\mathbf{V}, \mathbf{v}/\|\mathbf{v}\|]$
9: **end if**
10: **end for**
11: **end for**

Algorithm 2 Proposed Algorithm - Serial Version

1: $\mathbf{p} = \mathcal{S}_0$
2: Compute $\Sigma(\mathbf{s})\big|_{\mathbf{p}}$ according to (34a)
3: $\mathbf{V} = \mathrm{WCAWE}\left(\Sigma(\mathbf{s})\big|_{\mathbf{p}}, q\right)$
4: Compute $\tilde{\Sigma}(\mathbf{s})$ with $\mathbf{V}$
5: **for** $r = 1 \dots q$ **do**
6: **for** $\forall \mathbf{p} \in \tilde{\mathcal{S}}_r$ **do**
7: Compute $\tilde{\Sigma}(\mathbf{s})\big|_{\mathbf{p}}$ according to (34a)
8: $[\tilde{\mathbf{u}}_0 \dots \tilde{\mathbf{u}}_{r-1}] = \mathrm{WCAWE}\left(\tilde{\Sigma}(\mathbf{s})\big|_{\mathbf{p}}, r-1\right)$
9: $[\mathbf{u}_0 \dots \mathbf{u}_{r-1}] = \mathbf{V}\,[\tilde{\mathbf{u}}_0 \dots \tilde{\mathbf{u}}_{r-1}]$
10: $[\mathbf{u}_r \dots \mathbf{u}_q] = \mathrm{WCAWE}\left(\Sigma(\mathbf{s})\big|_{\mathbf{p}}, [\mathbf{u}_0 \dots \mathbf{u}_{r-1}], q\right)$
11: **for** $k = r \dots q$ **do**
12: $\mathbf{v} := \mathrm{MGS}\left(\mathbf{u}_k, \mathbf{V}\right)$
13: $\mathbf{V} := [\mathbf{V}, \mathbf{v}/\|\mathbf{v}\|]$
14: **end for**
15: **end for**
16: Compute $\tilde{\Sigma}(\mathbf{s})$ with $\mathbf{V}$
17: **end for**

1) Efficiency improvement: Beside the factorization of the system matrix, one of the most expensive steps during the computation of the multivariate basis is the construction of $[\mathbf{u}_0, \dots, \mathbf{u}_q]$ for each contraction direction. The dimension of the basis to be computed is given by (12). The number of vectors $\mathbf{u}_k(\mathbf{p})$ computed in Alg. 1 is

$$N_u = (q+1)\dim \mathcal{P}_q(m) = (q+1)\binom{q+m-1}{q}, \quad (45)$$

which exceeds (12). Many of the vectors with degree $r < q$ do not contribute to the basis $\mathbf{V}$. Their sole use is to provide the history needed by recursion (41) to compute the non-redundant basis vectors of higher order.

Since the redundant vectors $\mathbf{u}_r$ are linearly dependent to the column vectors of the already computed matrix $\mathbf{V}$, they need not to be computed by the WCAWE process on the full model in each contraction direction, but can be efficiently reconstructed from the known basis vectors. We propose to consider the ROM $\tilde{\Sigma}(\mathbf{s})$ built by projection with $\mathbf{V}$. Let $[\tilde{\mathbf{u}}_0, \dots, \tilde{\mathbf{u}}_r]$ denote the WCAWE vectors of contraction $\tilde{\Sigma}(\mathbf{s})\big|_{\mathbf{p}}$. The WCAWE vectors of the contracted original model can be reconstructed by means of

$$\begin{bmatrix}\mathbf{u}_0 & \dots & \mathbf{u}_r\end{bmatrix} = \mathbf{V}\begin{bmatrix}\tilde{\mathbf{u}}_0 & \dots & \tilde{\mathbf{u}}_r\end{bmatrix}. \quad (46)$$

Since numerical costs for the WCAWE iteration on the ROM can be neglected compared to the forward-back substitution on the original model, this constitutes a very efficient method for computing the linearly dependent vectors. To state the final algorithm, we first have to introduce the incremental sets of contraction directions $\tilde{\mathcal{S}}_r$:

$$\mathcal{S}_r = \tilde{\mathcal{S}}_r \oplus \mathcal{S}_{r-1}. \quad (47)$$

With this definition, the proposed method is given in Alg. 2. Note that in line 10 only WCAWE vectors with dimension of the full model need to be computed. Unfortunately, the efficiency gain of this approach complicates parallelization, since the computation of the WCAWE vectors in different contraction directions cannot be split into independent processes anymore. In [15] a similar approach was presented for the linearly parameterized case.

2) Direction-Dependent Choice of Model Order: According to (12), the dimension of the ROM increases very strong with the considered moment order q. In the method presented so far, the order of the ROM is equal for all parameters. In many applications in contrary, parameter ranges in some parameters are wide, e.g. usually the frequency, whereas other are rather small. These different requirements on bandwidth are only inadequately fulfilled by ROMs of homogeneous order.

Since our proposed method uses single-parameter systems, we can apply the error- and termination criteria developed for them, see e.g. [18] and [19, Chapter 5], to choose the order of the single-parameter systems direction-dependently.

V. Extensions

A. Nonzero Expansion Point

So far, we have just considered moment-matching about the origin, $\mathbf{s} = \mathbf{0}$. However, there are situations when a general expansion point $\mathbf{s}_0 \neq \mathbf{0}$ may be preferable, e.g. for efficiency reasons, or when $\mathbf{A}(\mathbf{s} = \mathbf{0})$ is singular.

To make the theory of Section III applicable to such cases, we represent $\mathbf{s}$ in the form

$$\mathbf{s} = \mathbf{s}_0 + \Delta\mathbf{s}. \quad (48)$$

B. MIMO Systems

The extension to multiple-input multiple-output (MIMO) systems is based on the fact that the k-th row of the l-th column of the transfer function of the MIMO system

$$\Big(\sum_{|\alpha|=0}^{|\alpha|\leq M} \mathbf{s}^\alpha \mathbf{A}_\alpha\Big)\mathbf{x}(\mathbf{s}) = \Big(\sum_{|\alpha|=0}^{|\alpha|\leq M} \mathbf{s}^\alpha \mathbf{B}_\alpha\Big)\mathbf{u}(\mathbf{s}) \quad (49a)$$

$$\mathbf{y}(\mathbf{s}) = \Big(\sum_{|\alpha|=0}^{|\alpha|\leq M} \mathbf{s}^\alpha \mathbf{C}_\alpha^T\Big)\mathbf{x}(\mathbf{s}) \quad (49b)$$

with $\mathbf{x} \in \mathbb{C}^N$, $\mathbf{u} \in \mathbb{C}^g$, $\mathbf{y} \in \mathbb{C}^h$, $\mathbf{A}_\alpha \in \mathbb{C}^{N\times N}$, $\mathbf{B}_\alpha \in \mathbb{C}^{N\times g}$, and $\mathbf{C}_\alpha \in \mathbb{C}^{h\times N}$, is identical to the transfer function of (5),

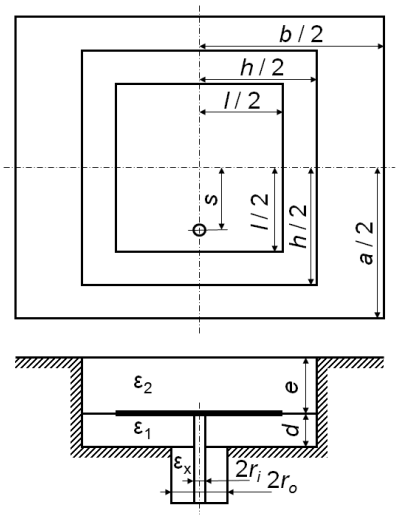

Fig. 1. Structure of patch antenna. Dimensions in mm: a=22.15, b=47.45, h=18.15, l=13.5, s=1.75, d=2.42, e=2.6, r_i=0.64, r_0=2.05.

provided that $\mathbf{b}_\alpha$ is the l-th column of $\mathbf{B}_\alpha$ and $\mathbf{c}_\alpha$ the k-th column of $\mathbf{C}_\alpha$, respectively. This implies that, in the MIMO case, the spaces in (30) just need to be replaced by the column spaces of the block vectors

$$\mathbf{X}_\beta = \mathbf{A}_{\alpha=0}^{-1}\Big(\mathbf{B}_\beta - \sum_{|\alpha|=1}^{|\alpha|\leq M} \mathbf{A}_\alpha \mathbf{B}_{\beta-\alpha}\Big) \tag{50a}$$

$$\mathbf{Z}_\beta = \mathbf{A}_{\alpha=0}^{-T}\Big(\mathbf{C}_\beta - \sum_{|\alpha|=1}^{|\alpha|\leq M} \mathbf{A}_\alpha^T \mathbf{Z}_{\beta-\alpha}\Big). \tag{50b}$$

VI. Numerical Examples

A. Patch Antenna

Fig. 1 shows the structure of the considered patch antenna [20]. We allow the reflection coefficient S_{11} to be a function of operation frequency f and the relative dielectric permittivities of the two substrate layers, ε_{r1} and ε_{r2}. A FE discretization with third order $H(\mathrm{curl})$-conforming shape functions [21] results in a parameterized system of the form

$$(\mathbf{S} + jk_0\mathbf{R} - k_0^2\mathbf{T} - \varepsilon_{r1}k_0^2\mathbf{T}_1 - \varepsilon_{r2}k_0^2\mathbf{T}_2)\mathbf{x} = jk_0\eta_0\mathbf{b} \tag{51a}$$

$$z = \mathbf{b}^T\mathbf{x}, \tag{51b}$$

where $k_0 = 2\pi f/c_0$ denotes the wave number. Note that the output of (51) is the input impedance, from which the reflection coefficient can be easily computed. The expansion point is set at $(\overline{f} = 6\ \text{GHz}, \overline{\varepsilon_{r1}} = 4, \overline{\varepsilon_{r2}} = 4)$. The original model (51) consists of $N = 368\,241$ degrees of freedom. The order of the ROM is chosen to be $q = 8$. According to (12) this results in a ROM dimension of 165. Figs. 2, 3 and 4 show the magnitude of S_{11} as a function of frequency and relative electric permittivity ε_{r1} for $\varepsilon_{r2} = 1$, $\varepsilon_{r2} = 4$, and $\varepsilon_{r2} = 7$, respectively. Note that each surface plot consists of $201 \times 201 = 40401$ model evaluations. To assess the accuracy of the new approach we present in Fig. 5 a comparison with the original model and method [16]. Fig. 6 shows the errors

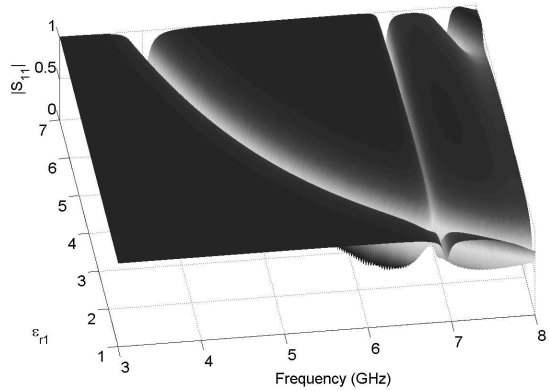

Fig. 2. Patch antenna. Magnitude of reflection coefficient at $\varepsilon_{r2} = 1$ as a function of frequency and relative electric permittivity ε_{r1}.

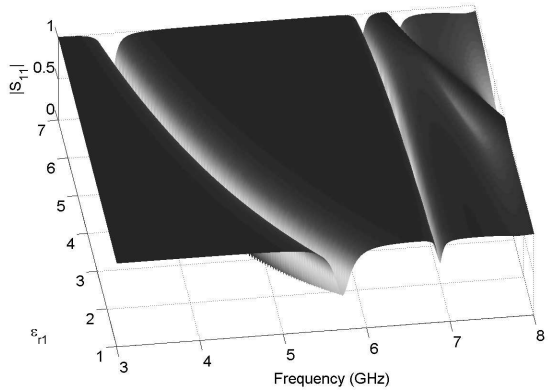

Fig. 3. Patch antenna. Magnitude of reflection coefficient at $\varepsilon_{r2} = 4$ as a function of frequency and relative electric permittivity ε_{r1}.

of the ROMs compared to the original model

$$|\text{Error}| = |S_{11}^{ROM} - S_{11}^{FE}|. \tag{52}$$

As can be clearly seen, the new approach leads to smaller errors in the reflection coefficient. Since the projection matrices of our proposed method and the approach presented in [16] are identical in the absence of round-off errors, this improvement can be contributed to increased numerical stability. Minor differences between Alg. 1 and 2 are due to numerical noise.

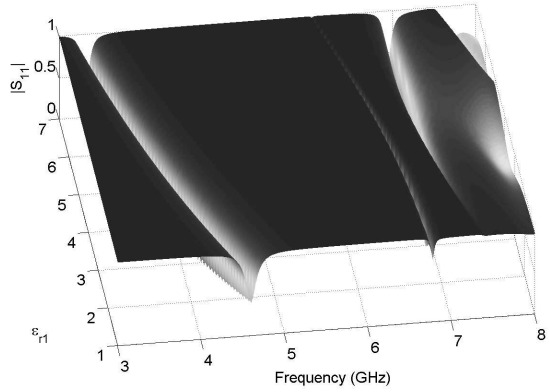

Fig. 4. Patch antenna. Magnitude of reflection coefficient at $\varepsilon_{r2} = 7$ as a function of frequency and relative electric permittivity ε_{r1}.

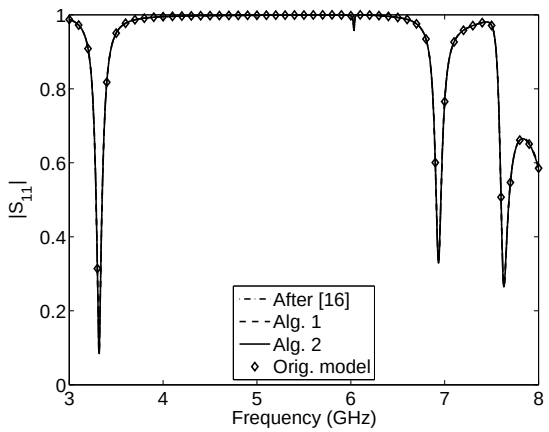

Fig. 5. Patch antenna. Magnitude of reflection coefficient as a function of frequency at $\varepsilon_{r1} = 7$, $\varepsilon_{r2} = 7$.

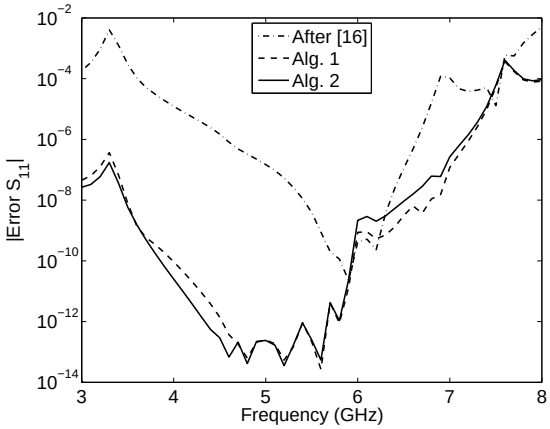

Fig. 6. Patch antenna. Magnitude of error in reflection coefficient as a function of frequency at $\varepsilon_{r1} = 7$, $\varepsilon_{r2} = 7$.

Table I shows the speed-up attainable by using Alg. 2 for model generation. The reduction in ROM generation time between Alg. 1 and Alg. 2 is approximately 9 percent. Both algorithms are substantially faster than the method of [16]. Comparing the evaluation times for ROM and original model, we observe a difference of more than four orders of magnitude. The ROM can be evaluated 90 times per second. For the surface plots of Figs. 2, 3 and 4 this means a reduction of computation times from more than 115 days for the original model to approximately 9 minutes for the ROM.

B. Circulator

Fig. 7 presents a circulator with a triangular ferrite post [22]. The relative permeability tensor of the ferrite is given by

$$\boldsymbol{\mu}_r = \begin{bmatrix} \mu_r & -j\kappa_r & 0 \\ j\kappa_r & \mu_r & 0 \\ 0 & 0 & 1 \end{bmatrix} \tag{53}$$

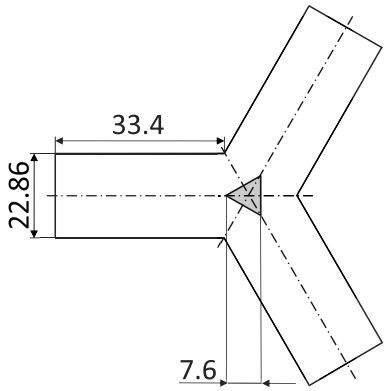

Fig. 7. Structure of Circulator. All dimensions are given in mm.

We now consider as parameters μ_r, κ_r and the frequency f. After discretization we end up with a system of the form

$$\Big(\mathbf{S}^{\bar{F}} + \frac{\mu_r}{\mu_r^2 - \kappa_r^2}\mathbf{S}_1^F + \frac{j\kappa_r}{\mu_r^2 - \kappa_r^2}\mathbf{S}_2^F + \mathbf{S}_3^F - k_0^2\mathbf{T}\Big)\mathbf{x} = jk_0\eta_0\mathbf{B} \tag{54a}$$

$$\mathbf{Z} = \mathbf{B}^T\mathbf{x}. \tag{54b}$$

The frequency dependent port normalization due to waveguide dispersion can be taken into account by an appropriate post processing step [23]. At first sight (54) does not fit into the framework of multivariate polynomially parameterized systems. But multiplication of (54a) with $(\mu_r^2 - \kappa_r^2)$ results in a system of the sought structure and our proposed order reduction method can be used. Normally μ_r and κ_r are themselves functions of the frequency [22]. Since we consider the three parameters independently from each other, we can take an arbitrary frequency dependence of the material properties into account by evaluating the ROM along the appropriate curve in the (f, μ_r, κ_r) space. Note that material property changes of a typical ferrite like TT1-109 lie in the ranges of $\mu_r = [0.966, 0.986] - j[7e-7, 4e-7]$, $\kappa_r = [0.3, 0.47] + j[4e8, 1e7]$ in the considered frequency range. In the following we will allow substantially larger parameter variations. The original model has a dimension of $N = 108\,935$. A ROM of order $q = 6$ results in a reduction to 252 degrees of freedom. The expansion point is set at ($\overline{f} = 10$ GHz, $\overline{\mu_r} = 3$, $\overline{\kappa_r} = 2$). Fig. 8 presents a two dimensional cut through the three dimensional response hypersurface at $\kappa_r = 0.37$. The surface plot again requires $40\,401$ model evaluations. Fig. 9 shows the frequency response of the system for $\mu_r = 1$ and $\kappa_r = 0.37$. Since $|S_{11}|$ and $|S_{13}|$ are below 30 dB around $f = 9.9$ GHz and $|S_{12}|$ is approximately one, the functionality of the structure as a circulator can by clearly observed. To demonstrate the correctness of the theory of Section III, we compare in Fig. 10 the accuracy of ROMs built from one sided and two sided projections. With this example, two sided projections lead to an increase in accuracy of one order of magnitude. Fig. 11 confirms the accuracy of all three order reduction algorithms in this particular case. To demonstrate the applicability of the proposed method even in the lossy case, Fig. 12 shows a comparison of original model and ROM at material parameters

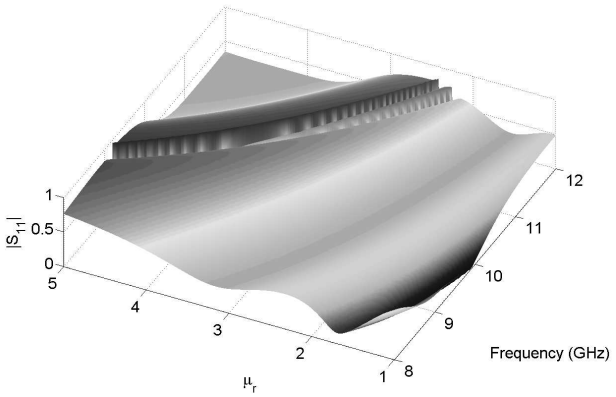

Fig. 8. Circulator. Magnitude of reflection coefficient at $\kappa_r = 0.37$ as a function of frequency and relative magnetic permeability μ_r.

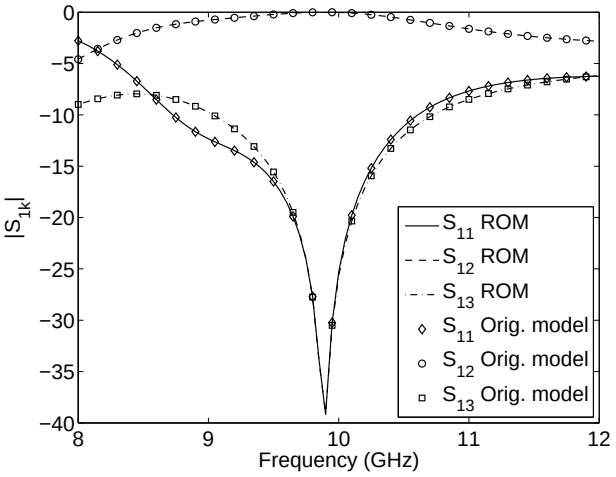

Fig. 9. Circulator. Magnitude of scattering parameters as a function of frequency at $\mu_r = 1$ and $\kappa_r = 0.37$. Alg. 1 is used to compute the ROM.

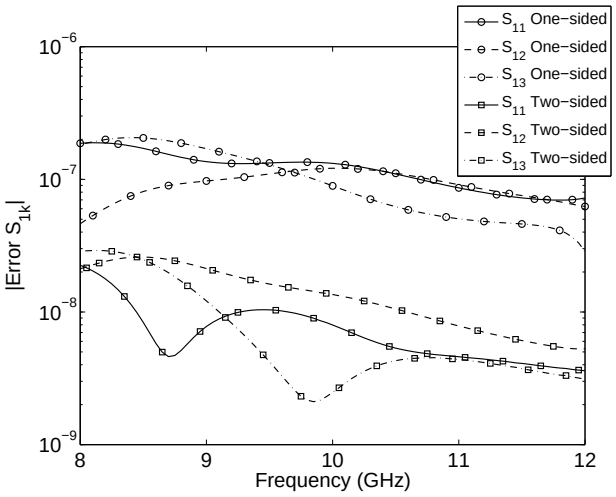

Fig. 10. Circulator. Comparison of ROMs using one sided or two sided projections. Magnitude of error in scattering parameters as a function of frequency at $\mu_r = 1$ and $\kappa_r = 0.37$. Alg. 1 is used to compute the ROM.

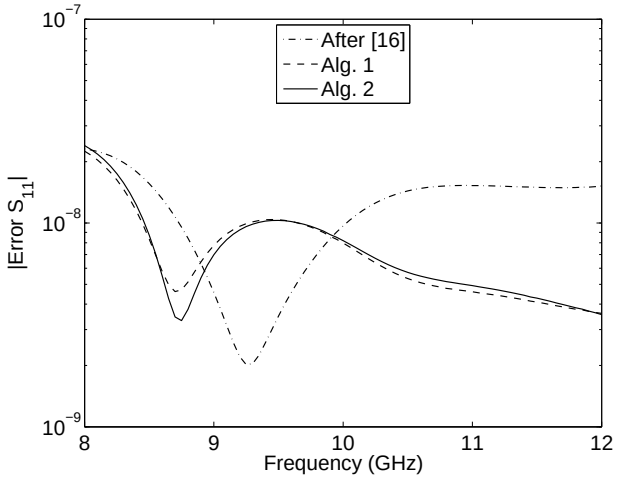

Fig. 11. Circulator. Comparison of ROMs built with different algorithms. Magnitude of error as a function of frequency at $\mu_r = 1$ and $\kappa_r = 0.37$.

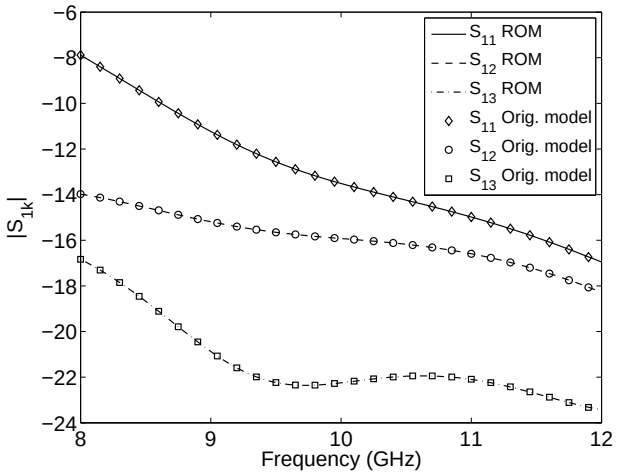

Fig. 12. Circulator. Magnitude of scattering parameters as a function of frequency at $\mu_r = 2 - 3j$ and $\kappa_r = 2 + 3j$. Alg. 1 is used to compute the ROM.

with a magnetic loss angle of more than $\delta = \pi/4$. The corresponding error plot in Fig. 13 again demonstrates the high fidelity of the ROM. The runtimes in Tab. I confirm the observations of Section VI-A: ROM generation using Alg. 1 and Alg. 2 is much faster than using method [16]. Alg. 2 is faster than Alg. 1. Evaluating the ROM is more than three order of magnitude faster than evaluating the original model.

VII. Conclusion

In this paper, we have extended the concept of polynomial moment-matching to the multi-parameter case. This includes parameterization, not only of the system matrix, but also of the input and output vectors. The analysis of the projection spaces has led to a new algorithm, which outperforms existing methods not only in numerical robustness, computational runtime and reduced memory consumption, but also allows as additional features a straightforward parallelization and the handling of non-uniform parameter ranges.

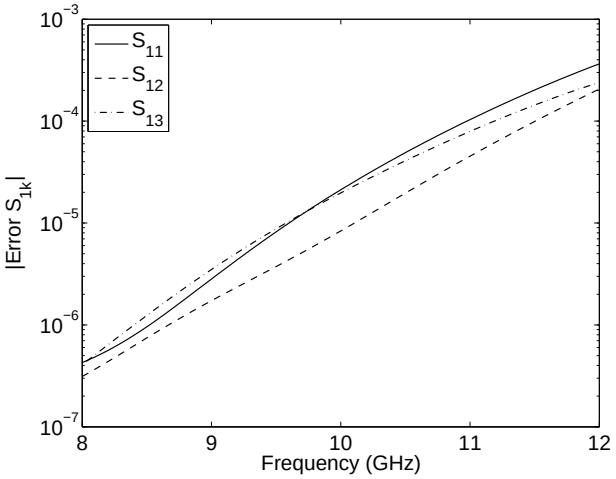

Fig. 13. Circulator. Magnitude of error in scattering parameters as a function of frequency at $\mu_r = 2 - 3j$ and $\kappa_r = 2 + 3j$. Alg. 1 is used to compute the ROM.

TABLE I
COMPUTATIONAL DATA[1]

	Patch antenna[2]	Circulator[3]
ROM Generation (s)		
After [16]	20015.65	15273.40
Algorithm 1	5077.70	2905.22
Algorithm 2	4631.14	2818.96
Model evaluation (s)		
ROM	$1.37 \cdot 10^{-2}$	$2.48 \cdot 10^{-2}$
Original model	246.00	34.93

[1] MATLAB implementation on AMD Opteron 250 processor, 2.39 GHz.
[2] Intel MKL PARDISO is used for solving sparse systems.
[3] MATLAB is used for solving sparse system.

APPENDIX A
PROOF OF (11)

Proof: Our starting point is the Taylor series (10). Plugging (10) into (7a) results in

$$\Big(\sum_{|\alpha|=0}^{|\alpha|\leq M} \mathbf{s}^\alpha \mathbf{A}_\alpha\Big)\Big(\sum_{|\beta|=0}^{\infty} \mathbf{x}_\beta \mathbf{s}^\beta\Big) = \sum_{|\alpha|=0}^{|\alpha|\leq M} \mathbf{s}^\alpha \mathbf{b}_\alpha \tag{55}$$

$$\sum_{|\alpha|=0}^{|\alpha|\leq M}\sum_{|\beta|=0}^{\infty} \mathbf{s}^{\alpha+\beta}\mathbf{A}_\alpha \mathbf{x}_\beta = \sum_{|\alpha|=0}^{|\alpha|\leq M} \mathbf{s}^\alpha \mathbf{b}_\alpha. \tag{56}$$

Applying the differential operator D^γ to (56) leads to

$$\sum_{|\alpha|=0}^{|\alpha|\leq M}\sum_{|\beta|=0}^{\infty} \frac{(\alpha+\beta)!}{(\alpha+\beta-\gamma)!}\mathbf{s}^{\alpha+\beta-\gamma}\mathbf{A}_\alpha \mathbf{x}_\beta = \sum_{|\alpha|=0}^{|\alpha|\leq M} \frac{\alpha!}{(\alpha-\gamma)!}\mathbf{s}^{\alpha-\gamma}\mathbf{b}_\alpha. \tag{57}$$

In the next step, we evaluate (57) at $\mathbf{s} = \mathbf{0}$. On the left-hand side, only summands with $\alpha + \beta - \gamma = 0$ remain, whereas, on the right-hand side, only terms with $\alpha - \gamma = 0$ give non-vanishing contributions. We therefore get

$$\sum_{|\alpha|=0}^{|\alpha|\leq M} \mathbf{A}_\alpha \mathbf{x}_{\gamma-\alpha} = \mathbf{b}_\gamma. \tag{58}$$

Solving for $\mathbf{x}_\gamma$ leads to the sought recursion

$$\mathbf{x}_\gamma = \mathbf{A}_{\alpha=0}^{-1}\Big(\mathbf{b}_\gamma - \sum_{|\alpha|=1}^{|\alpha|\leq M} \mathbf{A}_\alpha \mathbf{x}_{\gamma-\alpha}\Big). \tag{59}$$

■

APPENDIX B
PROOF OF LEMMA 3

Proof: The proof is by induction. For $\beta = 0$ we get

$$\begin{aligned}\tilde{\mathbf{x}}_{\beta=0} &= \tilde{\mathbf{A}}_{\alpha=0}^{-1}\tilde{\mathbf{b}}_{\beta=0} = \left(\mathbf{W}^T\mathbf{A}_{\alpha=0}\mathbf{V}\right)^{-1}\left(\mathbf{W}^T\mathbf{b}_{\beta=0}\right) \\ &= \left(\mathbf{W}^T\mathbf{A}_{\alpha=0}\mathbf{V}\right)^{-1}\mathbf{W}^T\mathbf{A}_{\alpha=0}\underbrace{\mathbf{A}_{\alpha=0}^{-1}\mathbf{b}_{\beta=0}}_{\mathbf{x}_{\beta=0}}.\end{aligned} \tag{60}$$

Since $\mathbf{x}_{\beta=0} = \mathbf{A}_{\alpha=0}^{-1}\mathbf{b}_{\beta=0} \in \mathrm{colsp}\{\mathbf{V}\}$, the following representation is possible

$$\mathbf{A}_{\alpha=0}^{-1}\mathbf{b}_{\beta=0} = \mathbf{V}\mathbf{c} \tag{61}$$

where $\mathbf{c} \in \mathbb{C}^m$. Plugging (61) in (60) gives

$$\tilde{\mathbf{x}}_{\beta=0} = \left(\mathbf{W}^T\mathbf{A}_{\alpha=0}\mathbf{V}\right)^{-1}\mathbf{W}^T\mathbf{A}_{\alpha=0}\mathbf{V}\mathbf{c} = \mathbf{c}. \tag{62}$$

Multiplying (62) by $\mathbf{V}$ proves the assumption for $\beta = 0$

$$\mathbf{V}\tilde{\mathbf{x}}_{\beta=0} = \mathbf{V}\mathbf{c} = \mathbf{x}_{\beta=0}. \tag{63}$$

In the induction step we have

$$\begin{aligned}\tilde{\mathbf{x}}_\beta &= \tilde{\mathbf{A}}_{\alpha=0}^{-1}\Big(\tilde{\mathbf{b}}_\beta - \sum_{|\alpha|=1}^{|\alpha|\leq M} \tilde{\mathbf{A}}_\alpha \tilde{\mathbf{x}}_{\beta-\alpha}\Big) \\ &= \left(\mathbf{W}^T\mathbf{A}_{\alpha=0}\mathbf{V}\right)^{-1}\mathbf{W}^T\Big(\mathbf{b}_\beta - \sum_{|\alpha|=1}^{|\alpha|\leq M} \mathbf{A}_\alpha \mathbf{V}\tilde{\mathbf{x}}_{\beta-\alpha}\Big).\end{aligned} \tag{64}$$

Assuming that the hypothesis holds for $\mathbf{x}_\gamma$ with $|\gamma| \leq |\beta| - 1$, we get

$$\begin{aligned}\tilde{\mathbf{x}}_\beta &= \left(\mathbf{W}^T\mathbf{A}_{\alpha=0}\mathbf{V}\right)^{-1}\mathbf{W}^T\Big(\mathbf{b}_\beta - \sum_{|\alpha|=1}^{|\alpha|\leq M} \mathbf{A}_\alpha \mathbf{x}_{\beta-\alpha}\Big) \\ &= \left(\mathbf{W}^T\mathbf{A}_{\alpha=0}\mathbf{V}\right)^{-1}\mathbf{W}^T\mathbf{A}_{\alpha=0} \\ &\qquad \underbrace{\mathbf{A}_{\alpha=0}^{-1}\Big(\mathbf{b}_\beta - \sum_{|\alpha|=1}^{|\alpha|\leq M} \mathbf{A}_\alpha \mathbf{x}_{\beta-\alpha}\Big)}_{\mathbf{x}_\beta}.\end{aligned} \tag{65}$$

Using precondition (21), we can state

$$\mathbf{A}_{\alpha=0}^{-1}\Big(\mathbf{b}_\beta - \sum_{|\alpha|=1}^{|\alpha|\leq M} \mathbf{A}_\alpha \mathbf{x}_{\beta-\alpha}\Big) = \mathbf{V}\mathbf{g}. \tag{66}$$

Plugging (66) into (65) yields

$$\tilde{\mathbf{x}}_\beta = \left(\mathbf{W}^T\mathbf{A}_{\alpha=0}\mathbf{V}\right)^{-1}\mathbf{W}^T\mathbf{A}_{\alpha=0}\mathbf{V}\mathbf{g} = \mathbf{g}. \tag{67}$$

We next multiply (67) with $\mathbf{V}$ and get the desired result

$$\mathbf{V}\tilde{\mathbf{x}}_\beta = \mathbf{V}\mathbf{g} = \mathbf{x}_\beta. \tag{68}$$

■

APPENDIX C
PROOF OF THEOREM 5

Proof: To proof moment-matching up to order $q+p+1$, we have to show that for the difference of the Taylor series expansions of the transfer function of original and reduced model the following relation holds:

$$\epsilon(\mathbf{s}) = H(\mathbf{s}) - \tilde{H}(\mathbf{s}) = \mathcal{O}(\mathbf{s}^\beta), \quad \text{with } |\beta| = q+p+2. \tag{69}$$

Using (18) and (25) we can write

$$\epsilon(\mathbf{s}) = \Big(\sum_{|\alpha|=0}^{|\alpha|\leq M} \mathbf{s}^\alpha \mathbf{c}_\alpha^T\Big)\mathbf{e}_\mathbf{x}(\mathbf{s}) = \mathbf{x}_t^T(\mathbf{s})\Big(\sum_{|\alpha|=0}^{|\alpha|\leq M} \mathbf{s}^\alpha \mathbf{A}_\alpha\Big)\mathbf{e}_\mathbf{x}(\mathbf{s}). \tag{70}$$

Let $\tilde{\mathbf{x}}_t(\mathbf{s})$ denote the solution vector of the transposed system to ROM (13). The application of Lemma 3 to the transposed system gives

$$\mathbf{x}_t(\mathbf{s}) = \mathbf{W}\tilde{\mathbf{x}}_t(\mathbf{s}) + \mathbf{e}_{\mathbf{x}_t}(\mathbf{s}) \tag{71}$$

with

$$\|\mathbf{e}_{\mathbf{x}_t}(\mathbf{s})\| = \mathcal{O}(\mathbf{s}^\beta), \quad \text{with } |\beta| = p+1. \tag{72}$$

Plugging (71) into (70), we arrive at

$$\epsilon(\mathbf{s}) = \Big(\mathbf{W}\tilde{\mathbf{x}}_t(\mathbf{s}) + \mathbf{e}_{\mathbf{x}_t}(\mathbf{s})\Big)^T\Big(\sum_{|\alpha|=0}^{|\alpha|\leq M} \mathbf{s}^\alpha \mathbf{A}_\alpha\Big)\mathbf{e}_\mathbf{x}(\mathbf{s}). \tag{73}$$

With

$$\mathbf{W}^T\Big(\sum_{|\alpha|=0}^{|\alpha|\leq M} \mathbf{s}^\alpha \mathbf{A}_\alpha\Big)\mathbf{e}_\mathbf{x}(\mathbf{s}) = \mathbf{0} \tag{74}$$

which is the Petrov-Galerkin condition underlying ROM (13), we get with (72) and (23)

$$\begin{aligned}\epsilon(\mathbf{s}) &= \mathbf{e}_{\mathbf{x}_t}^T(\mathbf{s})\Big(\sum_{|\alpha|=0}^{|\alpha|\leq M} \mathbf{s}^\alpha \mathbf{A}_\alpha\Big)\mathbf{e}_\mathbf{x}(\mathbf{s}) \\ &= \mathcal{O}(\mathbf{s}^\beta), \quad \text{with } |\beta| = q+p+2. \end{aligned} \tag{75}$$

■

REFERENCES

[1] L. T. Pillage and R. A. Rohrer, "Asymptotic waveform evaluation for timing analysis," *IEEE Trans. Comput.-Aided Design Integr. Circuits Syst.*, vol. 33, no. 9, pp. 352–366, Apr 1990.

[2] D. S. Weile, E. Michielssen, E. Grimme, and K. Gallivan, "A method for generating rational interpolant reduced order models of two-parameter linear systems," *Applied Mathematics Letters*, vol. 12, pp. 93–102, Jul. 1999.

[3] P. Gunupudi, R. Khazaka, and M. Nakhla, "Analysis of transmission line circuits using multidimensional model reduction techniques," *IEEE Trans. Adv. Packag.*, vol. 25, no. 2, pp. 174–180, May 2002.

[4] C. Prud'homme, D. V. Rovas, K. Veroy, L. Machiels, Y. Maday, A. Patera, and G. Turinici, "Reliable real-time solution of parameterized partial differential equations: reduced-basis output bound methods," *Journal of Fluids Engineering*, vol. 124, pp. 70–80, 2002.

[5] J. E. Bracken, D.-K. Sun, and Z. J. Cendes, "S-domain methods for simultaneous time and frequency characterization of electromagnetic devices," *IEEE Trans. Microw. Theory Tech.*, vol. 46, no. 46, pp. 1277–1290, Sep. 1998.

[6] D. S. Weile and E. Michielssen, "Analysis of frequency selective surfaces using two-parameter generalized rational Krylov model-order reduction," *IEEE Trans. Antennas Propag.*, vol. 49, pp. 1539–1549, Nov. 2001.

[7] L. Daniel, O. C. Siong, L. S. Chay, K. H. Lee, and J. White, "A multiparameter moment-matching model-reduction approach for generating geometrically parameterized interconnect performance models," *IEEE Trans. Comput.-Aided Design Integr. Circuits Syst.*, vol. 23, pp. 678–693, May 2004.

[8] O. Farle, V. Hill, P. Nickel, and R. Dyczij-Edlinger, "Multivariate finite element model order reduction for permittivity or permeability estimation," *IEEE Trans. Magn.*, vol. 42, no. 4, pp. 623–626, Apr. 2006.

[9] P. Feldmann and R. W. Freund, "Efficient linear circuit analysis by padé approximation via the lanczos process," *IEEE Trans. Comput.-Aided Design Integr. Circuits Syst.*, vol. 34, pp. 639–649, May 1995.

[10] R. D. Slone, R. Lee, and J.-F. Lee, "Broadband model order reduction of polynomial matrix equation using single-point well-conditioned asymptotic waveform evaluation: Derivation and theory," *Int. J. Numer. Meth. Engng*, vol. 58, pp. 2325–2342, Dec. 2003.

[11] Z. Bai and Y. Su, "Dimension reduction of large-scale second-order dynamical systems via a second-order Arnoldi method," *SIAM Journal on Scientific Computing*, vol. 26, no. 5, pp. 1692–1709, 2005.

[12] P. K. Gunupudi, R. Khazaka, M. S. Nakhla, T. Smy, and D. Celo, "Passive parameterized time-domain macromodels for high-speed transmission-line networks," *IEEE Trans. Microw. Theory Tech.*, vol. 51, no. 12, pp. 2347–2354, Dec. 2003.

[13] L. H. Feng, E. B. Rudnyi, and J. G. Korvink, "Preserving the film coefficient as a parameter in the compact thermal model for fast electrothermal simulation," *IEEE Trans. Comput.-Aided Design Integr. Circuits Syst.*, vol. 24, no. 12, pp. 1838–1847, Dec. 2005.

[14] Y.-T. Li, Z. Bai, Y. Su, and X. Zeng, "Model order reduction of parameterized interconnect networks via a two-directional Arnoldi process," *IEEE Trans. Comput.-Aided Design Integr. Circuits Syst.*, vol. 27, no. 9, pp. 1571–1582, Sep. 2008.

[15] L. Codecasa, "A novel approach for generating boundary condition independent compact dynamic thermal networks of packages," *IEEE Transactions on Components and Packaging Technologies*, vol. 28, no. 4, pp. 593–604, Dec. 2005.

[16] O. Farle, V. Hill, P. Ingelström, and R. Dyczij-Edlinger, "Multi-parameter polynomial order reduction of linear finite element models," *Math. Comp. Model. Dyn. Sys., in press*, vol. 14, no. 5, pp. 421–434, 2008.

[17] G. A. Baker Jr. and P. Graves-Morris, *Padé Approximants*, 2nd ed. Cambridge University Press, 1996.

[18] Z. Bai, R. D. Slone, W. T. Smith, and Q. Ye, "Error bound for reduced system model by Pad´e approximation via the Lanczos process," *IEEE Trans. Comput.-Aided Design Integr. Circuits Syst.*, vol. 18, no. 2, pp. 133–141, Feb. 1999.

[19] E. Grimme, "Krylov projection methods for model reduction," Ph.D. dissertation, Coordinated-Science Laboratory, Univ. of Illinois at Urbana-Champaign, Urbana-Champaign, IL, 1997.

[20] M. A. G. de Aza, J. A. Encinar, J. Zapata, and M. Lambea, "Full-wave analysis of cavity-backed and probe-fed microstrip patch arrays by a hybrid mode-matching generalized scattering matrix and finite-element method," *IEEE Trans. Microw. Theory Tech.*, vol. 46, no. 2, pp. 234–242, Feb. 1998.

[21] P. Ingelström, "A new set of H(curl)-conforming hierarchical basis functions for tetrahedral meshes," *IEEE Trans. Microw. Theory Tech.*, vol. 54, no. 1, pp. 106–114, Jan. 2006.

[22] M. Koshiba and M. Suzuki, "Finite-element analysis of H-plane waveguide junction with arbitrarily shaped ferrite post," *IEEE Trans. Microw. Theory Tech.*, vol. 34, no. 1, pp. 103–109, Jan. 1986.

[23] J. Rubio, J. Arroyo, and J. Zapata, "SFELP-an efficient methodology for microwave circuit analysis," *IEEE Trans. Microw. Theory Tech.*, vol. 49, no. 3, pp. 509–516, Mar. 2001.